https://doi.org/10.5194/egusphere-2025-906
Preprint. Discussion started: 7 March 2025

Brief communication: Correction of Fundamental Errors in the EVP Sea Ice Dynamics in ICON

Oliver Gutjahr[1]

[1]Department of Environmental Meteorology, Trier University, Trier, Germany

Correspondence: Oliver Gutjahr (gutjahr@uni-trier.de)

Abstract. Since its implementation, EVP sea ice dynamics in the ice-ocean model ICON-O contained severe errors and thus all ICON simulations coupled to it. Two errors prevented convergence of the EVP solver, while a third miscalculated the quadratic drag law using an incorrect relative ice velocity. This caused excessive ice drift, overly mobile ice, and large open water patches, distorting ocean-atmosphere exchanges—worsening at higher resolutions. Correcting them improved the sea ice drift, aligning it with observations and yielding a realistic ice cover. This study marks a turning point in ICON's sea ice representation, ensuring significantly improved simulations at all resolutions.

1 Introduction

Sea ice is a key component of the Earth's climate system, playing a crucial role in the global energy balance, ocean circulation, and ecosystem dynamics (Stroeve and Notz, 2018). Accurately simulating sea ice in Earth system models is essential for understanding past climate variability, monitoring current trends, and making reliable projections of future climate change.

Sea ice motion is governed by external forcing from the atmosphere and ocean that exert stress on the sea ice, whereas internal rheology determines its deformation (Hibler, 1979). Small inaccuracies in the implementation of sea ice dynamics in numerical models can introduce significant biases in sea ice extent, thickness, and motion. These biases affect the energy and momentum exchange with the atmosphere and ocean, leading to errors in weather and climate simulations.

The Icosahedral Non-hydrostatic model (ICON, Jungclaus et al., 2022; Hohenegger et al., 2023) is used for a variety of climate and weather applications, including coupled simulations within the Coupled Model Intercomparison Project Phase 6 (CMIP6) framework (Eyring et al., 2016) or nextGEMs (Segura et al., 2025). This study identifies and corrects three errors in the implementation of sea ice dynamics in the ocean-sea ice component of the ICON model, ICON-O (Korn, 2017; Korn et al., 2022). The impact of these errors is assessed through short simulations at the kilometer scale (5 km) with and without corrections, providing insight into their influence on simulated sea ice behavior.

https://doi.org/10.5194/egusphere-2025-906
Preprint. Discussion started: 7 March 2025

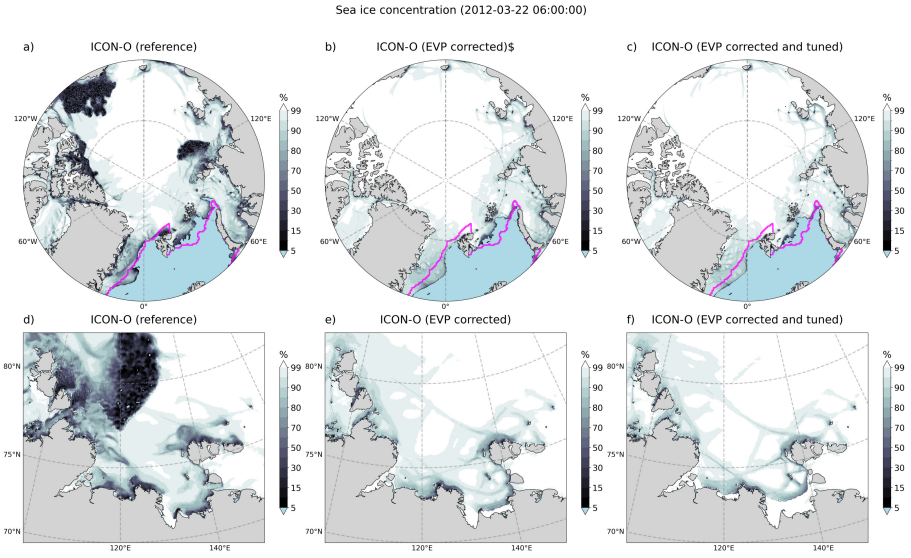

Figure 1. Effect of correcting and retuning the EVP sea ice dynamics in ICON-O on the sea ice concentration (6-hourly mean) in the Arctic Ocean with a) previous EVP dynamics with errors, b) corrected EVP dynamics, c) corrected and tuned EVP dynamics; and in the Laptev Sea (d-f). The magenta line marks the 15 % sea ice concentration from Ocean and Sea Ice Satellite Application Facility (OSI SAF, version 3) for the same day (Lavergne et al., 2019).

2 Identified errors and their corrections in the EVP sea ice dynamics in ICON-O

The previous implementation of the Elastic-Viscous-Plastic (EVP) sea ice dynamics (Hunke and Dukowicz, 1997) in ICON-O (release version 2024.10), adopted from the Finite-Element Sea Ice Model (FESIM, version 2) (Danilov et al., 2015), contained significant errors that prevented convergence of the EVP solver and misrepresented the relative sea ice velocity in the quadratic drag law of the ice-ocean stress term.

While an omission of momentum loss from the ocean beneath the sea ice was identified and corrected (Proske et al., 2024), these additional errors remained undetected. As a result, the simulated sea ice drift was excessively strong, causing overly mobile ice to fracture too easily, forming large open water patches where continuous sea ice cover was expected.

The three identified errors in the sea ice dynamics of ICON-O are as follows:

1. Error 1 (introduced 2013): The sea ice velocities were incorrectly reset to zero at each iteration of the EVP solver, preventing numerical convergence.

2. Error 2 (introduced 2023): Similar to Error 1, but applied to the stress tensor.

3. Error 3 (introduced 2013): The quadratic drag law (ice-ocean stress term τ_w) was incorrectly applied as

$$\tau_w = \rho_0 C_w \|\mathbf{u_w} - \mathbf{u}_{\text{ice}}\|_2 (\mathbf{u_w}) \quad (1)$$

https://doi.org/10.5194/egusphere-2025-906
Preprint. Discussion started: 7 March 2025

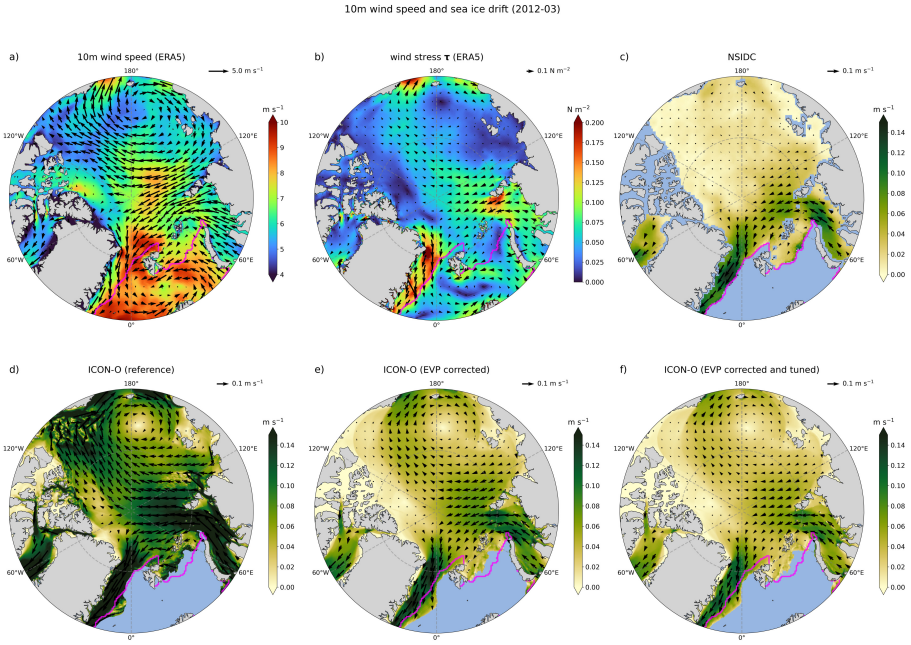

Figure 2. Effect of correcting and retuning the EVP sea ice dynamics in ICON-O on mean March 2012 sea ice drift in the Arctic Ocean: a) 10 m wind speed and b) wind stress from ERA5, c) sea ice drift from NSIDC, and ICON-O sea ice drift with d) erroneous EVP dynamics, e) corrected EVP dynamics, and f) corrected and tuned EVP dynamics. The magenta line marks the March 2012 mean 15 % sea ice concentration from OSI SAF (version 3) (Lavergne et al., 2019).

whereas the last term should have been $\mathbf{u_w} - \mathbf{u}_{\text{ice}}$. With ρ_0 a reference density, C_w the ice-ocean drag coefficient and u_w the ocean velocity.

The last error is also present in the recent version of FESOM2.5 (Rackow et al., 2025) and originated in ICON-O when the FESIM ice dynamics (Danilov et al., 2015) were adapted.

3 Impact assessment and simulations

3.1 ICON-O simulations at 5 km resolution

To assess the impact of the error and the improvements from their corrections, short (3-month) simulations were performed using the global uncoupled ICON-O model, based on the open release version 2024.10. The basic configuration is identical to that used in the nextGEMs project (Segura et al., 2025), as part of ICON-Sapphire (Hohenegger et al., 2023). ICON-O simulations were conducted at a horizontal resolution of approximately 5 km (R2B9) for January to March 2012, initialized from Ocean Reanalysis System 5 (ORAS5, Zuo et al., 2019). The surface wind stress and other atmospheric forcing is

https://doi.org/10.5194/egusphere-2025-906
Preprint. Discussion started: 7 March 2025

prescribed from hourly ERA5 (Hersbach et al., 2020). ICON-O uses a simple zero-layer thermodynamics model (Semtner, 1976) with one ice thickness class.

Three simulations were made: 1) a reference run with the erroneous EVP dynamics, 2) same as 1) but with corrected EVP dynamics, and 3) same as 2) but with tuned EVP dynamics. Since the EVP solver did not converge in previous versions, a tuning was necessary. Increasing the number of subiterations $N_{\mathrm{EVP}} = 500$ was found to be an appropriate balance between computational time and solution quality. The constant ice-ocean drag coefficient was raised to $C_w = 12 \times 10^{-3}$ (up from 5.5×10^{-3}) to counteract too strong wind stress from ERA5 (Hersbach et al., 2020) forcing, which assumes static ice conditions. It may need to be adjusted for coupled ICON simulations.

3.2 Impact of the corrected EVP sea ice dynamics

The first impact is on the sea ice concentration, which is exemplarily shown in Fig. 1 for a date (22. March 2012 at 6 UTC) near the end of the simulation. The simulation with the erroneous sea ice dynamics (Fig. 1a,d) produces large open water patches (Laptev Sea and Canadian Arctic), which are unrealistic and should not be confused with flaw polynyas typically observed at the transition between landfast and pack ice. After correcting the errors, the sea ice mobility was reduced as the EVP solver converged and the ice-ocean stress term was correctly applied, preventing the formation of large open water patches (Fig. 1b,e). Finally, retuning the ice-ocean drag coefficient and the number of subiterations in the EVP dynamics further improves the ice coverage (Fig. 1c), even producing some landfast sea ice in the Laptev Sea that was never observed in previous ICON-O simulations (Fig. 1f).

The second impact is on the drift speed of sea ice in ICON-O (Fig. 2). With the erroneous EVP dynamics (Fig. 2a), the sea ice drift is excessive compared to the National Snow and Ice Data Center (NSIDC) drift observations (version 4.1) (Tschudi et al., 2019) because ignoring the relative sea ice velocity reduces friction, which in turn accelerates the drift. After the correction, friction works as intended, significantly slowing down the drift (Fig. 2b). Since ERA5 overestimates the wind stress over sea ice, using a higher ice-ocean drag coefficient further slows the drift, which is in better agreement with NSIDC (Fig. 2c).

4 Conclusions

The identified errors in ICON's sea ice dynamics have been present since its initial implementation in 2013, with an additional error introduced in 2023. These errors affected all coupled ICON(-Sapphire) and standalone ICON-O simulations, with one error also affecting FESOM2.5 and earlier versions. The errors led to excessive sea ice drift and overly mobile sea ice that fractured too easily, forming large patches of open water. Consequently, incorrect momentum and energy exchanges with the atmosphere and ocean likely impacted the simulated weather and climate state.

With the corrected EVP sea ice dynamics, the simulated sea ice drift and compactness closely match the observations, avoiding unrealistic patches of open water and errors in the momentum and energy exchange with the atmosphere and the ocean. This study marks a turning point in ICON's sea ice representation, ensuring significantly improved simulations at all resolutions.

https://doi.org/10.5194/egusphere-2025-906
Preprint. Discussion started: 7 March 2025

Code and data availability. The ICON open-source code is available at https://gitlab.dkrz.de/icon/icon-model under a permissive open source license (https://opensource.org/license/BSD-3-clause). This study used release version 2024.10 (git hash a1324166fa60ec5bda5e838fdbfef4c19ae67899), which contains errors in the EVP sea ice dynamics. A corrected version of the ICON source code, including bug fixes for these EVP errors, can be found at https://doi.org/10.5281/zenodo.14912681 (Gutjahr, 2025a).

Interactive computing environment. The computing environment, including the Jupyter notebooks used for analysis and to produce the figures, is available at https://doi.org/10.5281/zenodo.14917934 (Gutjahr, 2025b).

Author contributions. OG has designed the study, made the corrections to the EVP sea ice dynamics in the ICON source code, conducted and analyzed the simulations, and wrote the manuscript.

Competing interests. The author declares no competing interests.

Acknowledgements. This research was funded by institutional resources of the Trier University and used resources of the Deutsches Klimarechenzentrum (DKRZ) granted by its Scientific Steering Committee (WLA) under project ID bb1470. Thanks to ICDC, CEN, University of Hamburg for data support. All plots and analysis were performed with Python version 3.10.10 (https://www.python.org/).

https://doi.org/10.5194/egusphere-2025-906
Preprint. Discussion started: 7 March 2025

References

Danilov, S., Wang, Q., Timmermann, R., Iakovlev, N., Sidorenko, D., Kimmritz, M., Jung, T., and Schröter, J.: Finite-Element Sea Ice Model (FESIM), version 2, Geoscientific Model Development, 8, 1747–1761, https://doi.org/10.5194/gmd-8-1747-2015, 2015.

Eyring, V., Bony, S., Meehl, G. A., Senior, C. A., Stevens, B., Stouffer, R. J., and Taylor, K. E.: Overview of the Coupled Model Intercomparison Project Phase 6 (CMIP6) experimental design and organization., Geosci. Model Dev., 9, 1937–1958, https://doi.org/10.5194/gmd-9-1937-2016, 2016.

Gutjahr, O.: ICON EVP Sea Ice Dynamics: Source Code and Corrections, https://doi.org/10.5281/zenodo.14912681, 2025a.

Gutjahr, O.: ICON EVP Sea Ice Dynamics: Jupyter Notebooks and Data, https://doi.org/10.5281/zenodo.14917934, 2025b.

Hersbach, H., Bell, B., Berrisford, P., Hirahara, S., Horányi, A., Muñoz-Sabater, J., Nicolas, J., Peubey, C., Radu, R., Schepers, D., Simmons, A., Soci, C., Abdalla, S., Abellan, X., Balsamo, G., Bechtold, P., Biavati, G., Bidlot, J., Bonavita, M., De Chiara, G., Dahlgren, P., Dee, D., Diamantakis, M., Dragani, R., Flemming, J., Forbes, R., Fuentes, M., Geer, A., Haimberger, L., Healy, S., Hogan, R. J., Hólm, E., Janisková, M., Keeley, S., Laloyaux, P., Lopez, P., Lupu, C., Radnoti, G., de Rosnay, P., Rozum, I., Vamborg, F., Villaume, S., and Thépaut, J.-N.: The ERA5 global reanalysis, Quarterly Journal of the Royal Meteorological Society, 146, 1999–2049, https://doi.org/https://doi.org/10.1002/qj.3803, 2020.

Hibler, W. D.: A Dynamic Thermodynamic Sea Ice Model, Journal of Physical Oceanography, 9, 815–846, https://doi.org/https://doi.org/10.1175/1520-0485(1979)009<0815:ADTSIM>2.0.CO;2, 1979.

Hohenegger, C., Korn, P., Linardakis, L., Redler, R., Schnur, R., Adamidis, P., Bao, J., Bastin, S., Behravesh, M., Bergemann, M., Biercamp, J., Bockelmann, H., Brokopf, R., Brüggemann, N., Casaroli, L., Chegini, F., Datseris, G., Esch, M., George, G., Giorgetta, M., Gutjahr, O., Haak, H., Hanke, M., Ilyina, T., Jahns, T., Jungclaus, J., Kern, M., Klocke, D., Kluft, L., Kölling, T., Kornblueh, L., Kosukhin, S., Kroll, C., Lee, J., Mauritsen, T., Mehlmann, C., Mieslinger, T., Naumann, A. K., Paccini, L., Peinado, A., Praturi, D. S., Putrasahan, D., Rast, S., Riddick, T., Roeber, N., Schmidt, H., Schulzweida, U., Schütte, F., Segura, H., Shevchenko, R., Singh, V., Specht, M., Stephan, C. C., von Storch, J.-S., Vogel, R., Wengel, C., Winkler, M., Ziemen, F., Marotzke, J., and Stevens, B.: ICON-Sapphire: simulating the components of the Earth system and their interactions at kilometer and subkilometer scales, Geoscientific Model Development, 16, 779–811, https://doi.org/10.5194/gmd-16-779-2023, 2023.

Hunke, E. C. and Dukowicz, J. K.: An Elastic–Viscous–Plastic Model for Sea Ice Dynamics, Journal of Physical Oceanography, 27, 1849–1867, https://doi.org/https://doi.org/10.1175/1520-0485(1997)027<1849:AEVPMF>2.0.CO;2, 1997.

Jungclaus, J. H., Lorenz, S. J., Schmidt, H., Brovkin, V., Brüggemann, N., Chegini, F., Crüger, T., De-Vrese, P., Gayler, V., Giorgetta, M. A., Gutjahr, O., Haak, H., Hagemann, S., Hanke, M., Ilyina, T., Korn, P., Kröger, J., Linardakis, L., Mehlmann, C., Mikolajewicz, U., Müller, W. A., Nabel, J. E. M. S., Notz, D., Pohlmann, H., Putrasahan, D. A., Raddatz, T., Ramme, L., Redler, R., Reick, C. H., Riddick, T., Sam, T., Schneck, R., Schnur, R., Schupfner, M., von Storch, J.-S., Wachsmann, F., Wieners, K.-H., Ziemen, F., Stevens, B., Marotzke, J., and Claussen, M.: The ICON Earth System Model Version 1.0, Journal of Advances in Modeling Earth Systems, 14, e2021MS002 813, https://doi.org/https://doi.org/10.1029/2021MS002813, e2021MS002813 2021MS002813, 2022.

Korn, P.: Formulation of an unstructured grid model for global ocean dynamics, J. Comp. Physiol., 339, 525–552, https://doi.org/10.1016/j.jcp.2017.03.009, 2017.

Korn, P., Brüggemann, N., Jungclaus, J. H., Lorenz, S. J., Gutjahr, O., Haak, H., Linardakis, L., Mehlmann, C., Mikolajewicz, U., Notz, D., Putrasahan, D. A., Singh, V., von Storch, J.-S., Zhu, X., and Marotzke, J.: ICON-O: The Ocean Component of the ICON Earth

https://doi.org/10.5194/egusphere-2025-906
Preprint. Discussion started: 7 March 2025

System Model—Global Simulation Characteristics and Local Telescoping Capability, Journal of Advances in Modeling Earth Systems, 14, e2021MS002 952, https://doi.org/https://doi.org/10.1029/2021MS002952, 2022.

Lavergne, T., Sørensen, A. M., Kern, S., Tonboe, R., Notz, D., Aaboe, S., Bell, L., Dybkjær, G., Eastwood, S., Gabarro, C., Heygster, G., Killie, M. A., Brandt Kreiner, M., Lavelle, J., Saldo, R., Sandven, S., and Pedersen, L. T.: Version 2 of the EUMETSAT OSI SAF and ESA CCI sea-ice concentration climate data records, The Cryosphere, 13, 49–78, https://doi.org/10.5194/tc-13-49-2019, 2019.

Proske, U., Brüggemann, N., Gärtner, J. P., Gutjahr, O., Haak, H., Putrasahan, D., and Wieners, K.-H.: A case for open communication of bugs in climate models, made with ICON version 2024.01, EGUsphere, 2024, 1–30, https://doi.org/10.5194/egusphere-2024-3493, 2024.

Rackow, T., Pedruzo-Bagazgoitia, X., Becker, T., Milinski, S., Sandu, I., Aguridan, R., Bechtold, P., Beyer, S., Bidlot, J., Boussetta, S., Deconinck, W., Diamantakis, M., Dueben, P., Dutra, E., Forbes, R., Ghosh, R., Goessling, H. F., Hadade, I., Hegewald, J., Jung, T., Keeley, S., Kluft, L., Koldunov, N., Koldunov, A., Kölling, T., Kousal, J., Kühnlein, C., Maciel, P., Mogensen, K., Quintino, T., Polichtchouk, I., Reuter, B., Sármány, D., Scholz, P., Sidorenko, D., Streffing, J., Sützl, B., Takasuka, D., Tietsche, S., Valentini, M., Vannière, B., Wedi, N., Zampieri, L., and Ziemen, F.: Multi-year simulations at kilometre scale with the Integrated Forecasting System coupled to FESOM2.5 and NEMOv3.4, Geoscientific Model Development, 18, 33–69, https://doi.org/10.5194/gmd-18-33-2025, 2025.

Segura, H., Pedruzo-Bagazgoitia, X., Weiss, P., Müller, S. K., Rackow, T., Lee, J., Dolores-Tesillos, E., Benedict, I., Aengenheyster, M., Aguridan, R., Arduini, G., Baker, A. J., Bao, J., Bastin, S., Baulenas, E., Becker, T., Beyer, S., Bockelmann, H., Brüggemann, N., Brunner, L., Cheedela, S. K., Das, S., Denissen, J., Dragaud, I., Dziekan, P., Ekblom, M., Engels, J. F., Esch, M., Forbes, R., Frauen, C., Freischem, L., García-Maroto, D., Geier, P., Gierz, P., González-Cervera, A., Grayson, K., Griffith, M., Gutjahr, O., Haak, H., Hadade, I., Haslehner, K., ul Hasson, S., Hegewald, J., Kluft, L., Koldunov, A., Koldunov, N., Kölling, T., Koseki, S., Kosukhin, S., Kousal, J., Kuma, P., Kumar, A. U., Li, R., Maury, N., Meindl, M., Milinski, S., Mogensen, K., Niraula, B., Nowak, J., Praturi, D. S., Proske, U., Putrasahan, D., Redler, R., Santuy, D., Sármány, D., Schnur, R., Scholz, P., Sidorenko, D., Spät, D., Sützl, B., Takasuka, D., Tompkins, A., Uribe, A., Valentini, M., Veerman, M., Voigt, A., Warnau, S., Wachsmann, F., Wacławczyk, M., Wedi, N., Wieners, K.-H., Wille, J., Winkler, M., Wu, Y., Ziemen, F., Zimmermann, J., Bender, F. A.-M., Bojovic, D., Bony, S., Bordoni, S., Brehmer, P., Dengler, M., Dutra, E., Faye, S., Fischer, E., van Heerwaarden, C., Hohenegger, C., Järvinen, H., Jochum, M., Jung, T., Jungclaus, J. H., Keenlyside, N. S., Klocke, D., Konow, H., Klose, M., Malinowski, S., Martius, O., Mauritsen, T., Mellado, J. P., Mieslinger, T., Mohino, E., Pawłowska, H., Peters-von Gehlen, K., Sarré, A., Sobhani, P., Stier, P., Tuppi, L., Vidale, P. L., Sandu, I., and Stevens, B.: nextGEMS: entering the era of kilometer-scale Earth system modeling, EGUsphere, 2025, 1–39, https://doi.org/10.5194/egusphere-2025-509, 2025.

Semtner, A. J.: A Model for the Thermodynamic Growth of Sea Ice in Numerical Investigations of Climate, Journal of Physical Oceanography, 6, 379–389, https://doi.org/https://doi.org/10.1175/1520-0485(1976)006<0379:AMFTTG>2.0.CO;2, 1976.

Stroeve, J. and Notz, D.: Changing state of Arctic sea ice across all seasons, Environmental Research Letters, 13, 103 001, https://doi.org/10.1088/1748-9326/aade56, 2018.

Tschudi, M., Meier, W. N., Stewart, J. S., Fowler, C., and Maslanik, J.: Polar Pathfinder Daily 25 km EASE-Grid Sea Ice Motion Vectors, Version 4, https://doi.org/10.5067/INAWUWO7QH7B, 2019.

Zuo, H., Balmaseda, M. A., Tietsche, S., Mogensen, K., and Mayer, M.: The ECMWF operational ensemble reanalysis–analysis system for ocean and sea ice: a description of the system and assessment, Ocean Science, 15, 779–808, https://doi.org/10.5194/os-15-779-2019, 2019.